Dynamics of Na + (Benzene) + Benzene Association and Ensuing Na + (Benzene) 2 * Dissociation

ARTICLE *in* THE JOURNAL OF PHYSICAL CHEMISTRY A · MAY 2015

Impact Factor: 2.69 · DOI: 10.1021/acs.jpca.5b01922 · Source: PubMed

3 AUTHORS, INCLUDING:

Amit Kumar Paul

Texas Tech University

24 PUBLICATIONS **119** CITATIONS

SEE PROFILE

Sujitha Kolakkandy

Texas Tech University

6 PUBLICATIONS **24** CITATIONS

SEE PROFILE

THE JOURNAL OF PHYSICAL CHEMISTRY A

Article

pubs.acs.org/JPCA

Dynamics of Na^+(Benzene) + Benzene Association and Ensuing $Na^+(Benzene)_2$* Dissociation

Amit K. Paul, Sujitha Kolakkandy, and William L. Hase*

Department of Chemistry and Biochemistry Texas Tech University, Lubbock, Texas 79409, United States

ABSTRACT: Chemical dynamics simulations were used to study Bz + Na^+(Bz) → $Na^+(Bz)_2$* association and the ensuing dissociation of the $Na^+(Bz)_2$* cluster (Bz = benzene). An interesting and unexpected reaction found from the simulations is direct displacement, for which the colliding Bz molecule displaces the Bz molecule attached to Na^+, forming Na^+(Bz). The rate constant for Bz + Na^+(Bz) association was calculated at 750 and 1000 K, and found to decrease with increase in temperature. By contrast, the direct displacement rate constant increases with temperature. The cross section and rate constant for direct displacement are approximately an order of magnitude lower than those for association. The $Na^+(Bz)_2$* cluster, formed by association, dissociates with a biexponential probability, with the rate constant for the short-time component approximately an order of magnitude larger than that for the longer time component. The latter rate constant agrees with that of Rice−Ramsperger−Kassel−Marcus (RRKM) theory, consistent with rapid intramolecular vibrational energy redistribution (IVR) and intrinsic RRKM dynamics for the $Na^+(Bz)_2$* cluster. A coupled phase space model was used to analyze the biexponential dissociation probability.

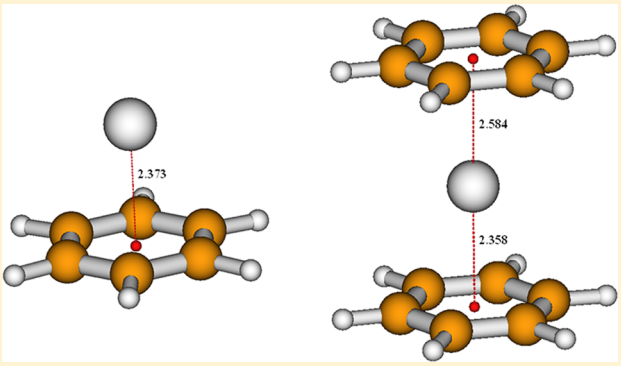

I. INTRODUCTION

The association of cations with polycyclic aromatic hydrocarbon (PAH) molecules is an interesting and important problem. The existence of PAH molecules in the interstellar medium and their possible role in forming clusters with iron atoms has been considered.[1−5] Many trace metals and their cations are present in hydrocarbon fuels, and they may participate in PAH coalescence, ultimately leading to soot formation.[6−14] From a fundamental perspective, it is important to understand the nature of cation−π interactions in metal cation−PAH clusters.

Both experimental and theoretical/computational studies have determined properties of clusters formed by the binding of aromatic molecules to metal cations.[15−33] This work has provided information regarding structures of the complexes, as well as the cation−aromatic binding energy. The theoretical/computational studies have given insights regarding the relative importance of electrostatic, polarization, charge transfer, and dispersion terms for binding of aromatics to the cation.[22,26−29] The computational studies have given values for the cation−aromatic intermolecular frequencies and shifts.[33]

The dynamics and kinetics of the formation of cation−aromatic molecule clusters by bimolecular association, and of the ensuing unimolecular dissociation of the clusters, have not been studied by either experiments, theory, or computation. For the work reported here, chemical dynamics simulations were performed to determine the cross section and rate constant for Na^+(Bz) + Bz association to form the vibrationally and rotationally excited $Na^+(Bz)_2$* cluster, and then analyze the unimolecular dissociation dynamics of this nonrandomly excited cluster. The goal of this work is to establish an understanding of the association and dissociation dynamics and kinetics of cation−aromatic molecule clusters. The dynamics of cations[34−38] and anions[39−41] associating with nonaromatic molecules has been investigated in previous computational studies.

II. COMPUTATIONAL PROCEDURE

A. Potential Energy Function. The analytic potential energy function for the Na^+(Bz) + Bz system is written as the sum[42]

$$V = V_{Bz} + V_{Bz,Bz} + V_{Na^+,Bz} \quad (1)$$

where V_{Bz} is the benzene intramolecular potential, $V_{Bz,Bz}$ is the benzene−benzene intermolecular potential, and $V_{Na^+,Bz}$ is the Na^+−benzene intermolecular potential. V_{Bz} is expressed in terms of Morse stretches, harmonic in-plane bends, harmonic out-of-plane wags, and torsions. The force constants for V_{Bz} are the same as those used previously.[43] For the Morse potentials, D_e is 125.8[44,45] and 116.4 kcal/mol[46,47] for the C−C and C−H bonds, respectively. The Morse parameter β_e is related to the harmonic force constant (f) by $\beta_e = (f/2D_e)^{1/2}$ and, respectively, is 1.95 and 1.78 $Å^{-1}$ for the C−C and C−H bonds.

Special Issue: 100 Years of Combustion Kinetics at Argonne: A Festschrift for Lawrence B. Harding, Joe V. Michael, and Albert F. Wagner

Received: February 26, 2015
Revised: April 30, 2015

DOI: 10.1021/acs.jpca.5b01922
J. Phys. Chem. A XXXX, XXX, XXX−XXX

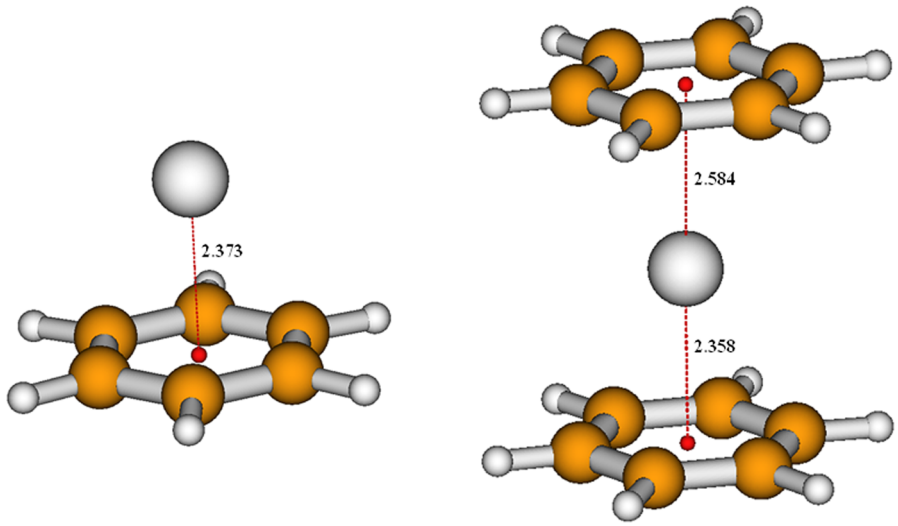

Figure 1. Equilibrium geometries of the $Na^+(Bz)$ and $Na^+(Bz)_2$ clusters for the analytic intermolecular potential as described in Section A. The distances are in angstrom.

The benzene−benzene intermolecular potential $V_{Bz,Bz}$ is represented by the OPLS model[48] for which the potential is written as a sum of two-body terms, each depending on r^{-12}, r^{-6}, and r^{-1}. The parameters for the two-body terms have been given and described previously.[48] The OPLS global minimum for the benzene dimer has a T-shaped geometry with a 2.32 kcal/mol classical binding energy and a Bz−Bz center-of-mass separation of 4.93 Å. A similar geometry with a 4.96 Å Bz−Bz separation and a binding energy of 2.84 kcal/mol is found from a CCSD(T)/CBS calculation.[49] The OPLS potential is expected to give an overall good description of the benzene−benzene intermolecular potential.

The OPLS potential was developed by fitting the 298 K heat of vaporization and density for liquid benzene, and the benzene dimer's ab initio structure and binding energy.[48] The potential gives values for liquid benzene's C−C radial distribution function and heat capacity which are in excellent agreement with experiment. Ab initio calculations have shown that molecular mechanical (MM) potentials like OPLS often do not accurately represent high energy repulsive regions of intermolecular potentials.[50,51] However, these regions should not be important for the 700 and 1000 K simulations reported here. Nevertheless, in future work it would be of interest to investigate the repulsive regions of the Bz−Bz OPLS potential.

The Na^+−Bz intermolecular potential was developed in previous work[42] by fitting MP2/6-311+G*calculations to two-body potentials of the form

$$V = A\exp(-Br) + \frac{C}{r^n} + \frac{D}{r^m} \tag{2}$$

to fit the Na^+−H and Na^+−C interactions. Values for the parameters A, B, C, D, n, and m for both interactions have been given previously.[42] MP2 potential energy curves, with both attractive and repulsive components, were calculated and fit for three Na^+ + Bz orientations; i.e., see Figure 1 of ref 42. This potential gives a $Na^+(Bz)$ binding energy of 25.5 kcal/mol compared to the MP2 value of 25.2 kcal/mol. The experimentally reported value is ∼22 kcal/mol.[24,25] The three $Na^+(Bz)$ intermolecular frequencies of 143, 143, 233 cm^{-1} for the analytic function are in quite good agreement with the MP2 values of 134, 134, and 208 cm^{-1}. The equilibrium geometries for the $Na^+(Bz)$ and $Na^+(Bz)_2$ clusters as obtained from the analytic potential are presented in Figure 1.

B. Chemical Dynamics Simulations. Chemical dynamics simulations were performed with the VENUS computer program,[52,53] to study $Na^+(Bz)$ + Bz → $Na^+(Bz)_2$ association and the ensuing decomposition of the vibrationally and rotationally excited $Na^+(Bz)_2$* cluster. The simulations were performed at fixed collision impact parameters and temperatures T of 750 and 1000 K for both $Na^+(Bz)$ and Bz. Quasiclassical sampling was used to add the 750 and 1000 K Boltzmann vibrational and rotational energy distributions to an ensemble of the collision partners.[54] Quantum harmonic oscillator distributions were sampled for the vibrational normal modes and classical rigid rotor distributions were sampled for the external rotational degrees of freedom. Standard algorithms were used to transform the vibrational and rotational energies of $Na^+(Bz)$ and Bz to Cartesian coordinates and momenta, and then the collision partners were randomly rotated. A relative center-of-mass collision energy of $3RT/2$ was then added to $Na^+(Bz)$ + Bz for a fixed collision impact parameter b. This approach, for simulating the temperature dependent dynamics, was tested for the 1000 K simulations by averaging over the relative collision energy distribution for the $Na^+(Bz)$ + Bz collisions.

For each ensemble with fixed b and T, 200 trajectories were calculated with a sixth-order symplectic integration algorithm.[55] The trajectories were integrated for either a maximum time of 90 ps or halted when the Na^+−Bz separation for the dissociating Bz molecue exceeded 20 Å. The integrations were performed with a time step of 0.5 fs, and energy was conserved to 1%, i.e., 0.20 kcal/mol. The properties determined from the trajectory simulations are the different types of trajectory events, the probability of forming the vibrationally and rotationally excited $Na^+(Bz)_2$* cluster versus impact parameter and temperature T, and the lifetime of these clusters.

III. SIMULATION RESULTS

Before presenting and discussing the trajectory results, it is useful to review the traditional statistical model[56,57] for $Na^+(Bz)$ + Bz association. It assumes $Na^+(Bz)$ + Bz collisions form the vibrationally/rotationally excited $Na^+(Bz)_2$* cluster, which then dissociates in accord with the Rice−Ramsperger−Kassel−

DOI: 10.1021/acs.jpca.5b01922
J. Phys. Chem. A XXXX, XXX, XXX−XXX

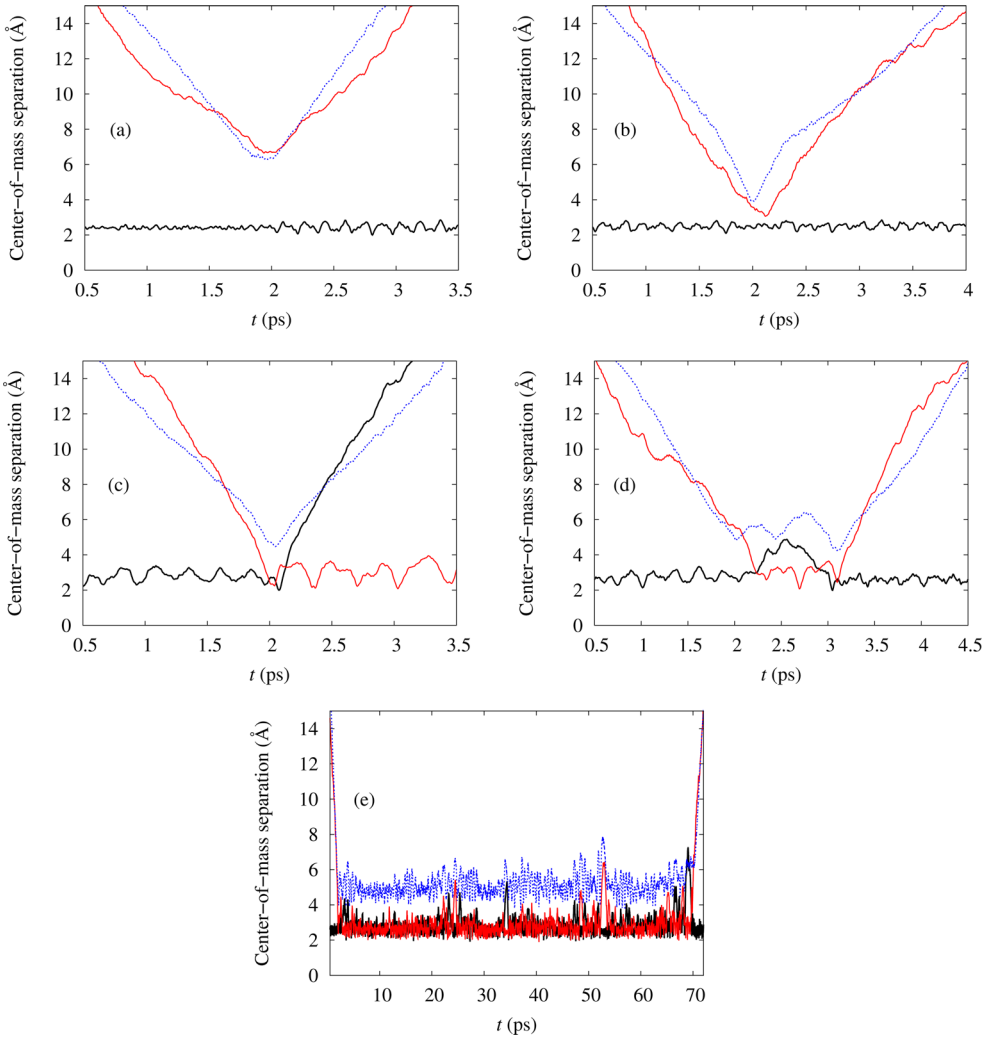

Figure 2. Illustrations of the different trajectory types for Bz2 + Na^+(Bz1): (a) direct scattering of Bz2, with the Na^+ and Bz2 separation remaining greater than 6 Å; (b) direct scattering with a short Na^+ and Bz2 separation; (c) direct displacement of Bz1 by Bz2, without cluster formation; (d) formation of a short-lived cluster with Bz2 dissociation; and (e) formation of a long-lived cluster with Bz2 dissociation. The black line is the Bz1−Na^+ distance, the red line the Bz2−Na^+ distance, and the dotted blue line the Bz1−Bz2 distance.

Marcus (RRKM) theory of unimolecular kinetics. As described below, two important nonstatistical dynamical features were found from the trajectories; i.e., a direct Na^+(Bz) + Bz displacement reaction without cluster formation and a nonexponential dissociation probability for the $Na^+(Bz)_2$* cluster.

A. Trajectory Types. The trajectories were classified as either association ($Na^+(Bz)_2$* cluster formation), direct displacement (the two Bz molecules were interchanged) or nonreactive. For trajectories, which did not form the cluster or undergo direct displacement, the colliding Bz molecule directly scattered off Na^+(Bz) without vibrating with respect to Na^+. For the majority of these trajectories, the Na^+−Bz separation for the colliding Bz remained greater than 6.0 Å, but for some Bz came very close to Na^+ without forming a $Na^+(Bz)_2$* cluster. These two trajectory types are illustrated in Figure 2a,b.

A small fraction of noncluster forming direct reactive trajectories were also found, for which the colliding Bz molecule directly displaces the Bz attached to Na^+; i.e., Bz + Na^+(Bz) → Na^+(Bz) + Bz. A representative trajectory is illustrated in Figure 2c.

The vibrationally/rotationally excited $Na^+(Bz)_2$*clusters, formed by Bz + Na^+(Bz) association, had a range of lifetimes as shown in Figure 2d and 2e. From an analysis of $Na^+(Bz)_2$* dissociation, it was found that, once the dissociating Bz molecule acquired a separation of 10 Å between its center-of-mass and Na^+, it dissociated and did not reform the cluster. Thus, the time the cluster dissociated was taken as the time a Na^+−Bz separation became 10 Å. A separation of 9 Å was not sufficient to identify dissociation. For each cluster formed, its lifetime was taken as the difference in the times the dissociation and initial association had a Na^+−Bz separation of 10 Å.

B. Bz + Na^+(Bz) →$Na^+(Bz)_2$* Association Probability, Cross Section, and Rate Constant. The association rate constant may be expressed as

$$k(T) = \int_0^\infty k(E_{rel})P(E_{rel})\,dE_{rel} \tag{3}$$

where $k(E_{rel})$, for Na^+(Bz) + Bz relative translational energy E_{rel}, is given by $k(E_{rel}) = v(E_{rel})\sigma(E_{rel})$ and $P(E_{rel})$ is the Boltzmann distribution for E_{rel}. $v(E_{rel})$ and $\sigma(E_{rel})$ are the relative velocity and association cross section, respectively. For calculating $\sigma(E_{rel})$, Na^+(Bz) has a Boltzmann distribution of vibrational and

DOI: 10.1021/acs.jpca.5b01922
J. Phys. Chem. A XXXX, XXX, XXX−XXX

rotational energies at T. Following previous work for ion−molecule association,[36] $k(E_{rel})$ is expressed as

$$k(E_{rel}) = a \exp(-bE_{rel}) \quad (4)$$

Inserting eq 4 into eq 3, $k(T)$ is analytic, i.e.,

$$k(T) = \left(\frac{1}{k_B T}\right)^{3/2} a\left(b + \frac{1}{k_B T}\right)^{-3/2} \quad (5)$$

An approximate expression for $k(T)$ is

$$k(T) \cong \nu(\bar{E}_{rel})\sigma(\bar{E}_{rel}) \quad (6)$$

where the ν and σ are calculated for the average relative translational energy $3k_BT/2$ for temperature T. For calculation of $\sigma(E_{rel})$, $Na^+(Bz)$ has a Boltzmann distribution of the vibrational and rotational energies at T. The $k(T)$ from eqs 5 and 6 are compared for the 1000 K simulations.

The probability of Bz + $Na^+(Bz)$ →$Na^+(Bz)_2$* association versus impact parameter b, i.e., $P_r(b)$, was calculated to determine the association cross section. To average over E_{rel} for the 1000 K simulations, $P_r(b)$ was calculated for E_{rel} of 1.0, 3.0, and 5.0 kcal/mol, where 3.0 kcal/mol is the average E_{rel} at 1000 K. The $P_r(b)$ for these three E_{rel} are plotted in Figure 3. The $P_r(b)$ for E_{rel} of 1.0 and 3.0 kcal/mol are simular, but the $P_r(b)$ are decidedly smaller for E_{rel} of 5.0 kcal/mol. For the 750 K simulations, $P_r(b)$ was only calculated for the average E_{rel} of $\bar{E}_{rel}$ = 2.2 kcal/mol and is also plotted in Figure 3. The $P_r(b)$ are similar for the 750 and 1000 K simulations at their $\bar{E}_{rel}$, except at the largest b $P_r(b)$ is somewhat larger for the lower temperature.

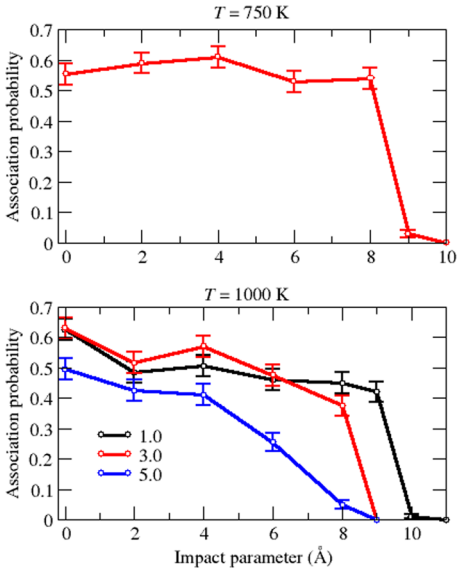

Figure 3. Probability of forming the $Na^+(Bz)_2$ cluster versus impact parameter b. The 1000 K simulations are performed for E_{rel} of 1.0, 3.0, and 5.0 kcal/mol, where 3.0 kcal/mol is the average E_{rel} at 1000 K. The 750 K simulations are only performed for E_{rel} of 2.2 kcal/mol, which is the average E_{rel} at this temperature. $Na^+(Bz)$ has a Boltzmann distribution of vibrational and rotational energies for both the 750 and 1000 K simulations.

Integrating $P_r(b)$ over the collision area $2\pi b$ for each impact parameter gives the collision cross section σ for association; i.e., $\sigma = \int P_r(b)2\pi b\, db$. Numerical integration gives σ equal to 132 ± 7.7, 106 ± 6.2, and 57.2 ± 4.2 Å^2 at E_{rel} of 1.0, 3.0, and 5.0 kcal/mol, respectively, for the simulations with T = 1000 K $Na^+(Bz)$ vibrational and rotational Boltzmann energy distributions. For the T = 750 K simulation, with $\bar{E}_{rel}$ of 2.2 kcal/mol, σ equals 128 ± 7.8 Å^2. Overall, the cross sections are precise with a standard deviation uncertainty of only ~6−7%.

To determine the 1000 K $k(T)$, from the three E_{rel} calculations, the resulting $k(E_{rel})$ were fit to eq 4 as shown in Figure 4. The fitting parameters are $a = 1.34 \times 10^{-9}$ cm^3/molecule·sec and b = 0.213 (kcal/mol)$^{-1}$. The value of $k(T)$ from eq 5 is (7.85 ± 0.47) × 10^{-10} cm^3/molecule·sec.

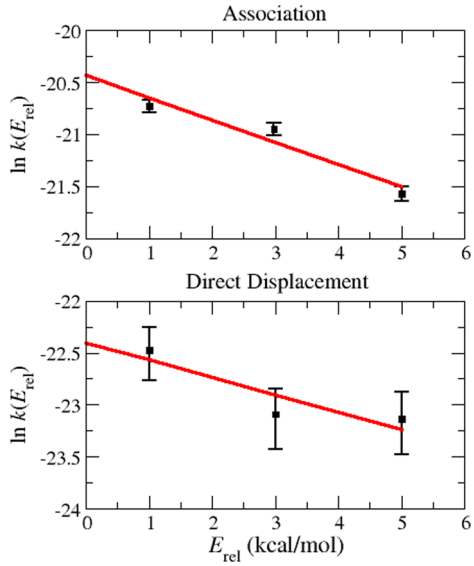

Figure 4. Plots of ln $k(E_{rel})$ versus E_{rel} for the association and direct displacement reactions. $Na^+(Bz)$ has a 1000 K Boltzmann distribution of vibrational and rotational energies. The plots are fit to eq 4. $k(E_{rel})$ is in units of cm^3/molecule·sec for E_{rel} of 1.0, 3.0, and 5.0 kcal/mol and is, respectively, 9.97 × 10^{-10}, 7.98 × 10^{-10}, and 4.30 × 10^{-10} for the association reaction and 17.4 × 10^{-11}, 9.37 × 10^{-11}, and 8.92 × 10^{-11} for the displacement reaction.

The 1000 K rate constant from eq 6 is (7.98 ± 0.48) × 10^{-10} cm^3/molecule·sec, which agrees with that from eq 5 within statistical uncertainty. Thus, eq 6 approximate expression for $k(T)$ gives an accurate value for the association rate constant. Equation 6 was used to determine $k(T)$ for 750 K and the value is 8.34 × 10^{-10} cm^3/molecule·sec.

Since the association $k(T)$ decreases with increase in T, the Arrhenius activation energy is negative. Using $k(T)$ determined for 750 and 1000 K from eq 6, gives E_a = −0.26 kcal/mol. The expression for E_a is analytic for $k(T)$ in eq 5 and is given by

$$E_a(T) = -\frac{3}{2}k_BT + \frac{3}{2}\left(b + \frac{1}{k_BT}\right)^{-1} \quad (7)$$

The resulting E_a is −0.88 kcal/mol at 1000 K, using the above parameter for b.

C. Bz + $Na^+(Bz)$ → $Na^+(Bz)$ + Bz Direct Displacement Probability, Cross Section, and Rate Constant. The dynamics for the $Na^+(Bz)$ + Bz direct displacement reaction were analyzed similar to the description given above for the $Na^+(Bz)$ + Bz association reaction. The displacement probabilities versus impact parameter, $P_r(b)$, determined from the simulations are plotted in Figure 5. The 750 K simulation is performed at $\bar{E}_{rel}$ = 2.2 kcal/mol, the average relative translational energy at 750 K. Calculations are performed at E_{rel} of 1.0, 3.0, and

DOI: 10.1021/acs.jpca.5b01922
J. Phys. Chem. A XXXX, XXX, XXX−XXX

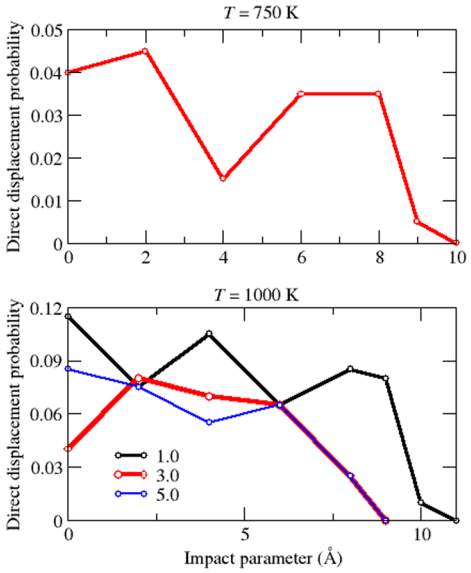

Figure 5. Same as Figure 3, but the probability of the Bz2 + $Na^+(Bz1) \rightarrow Na^+(Bz2)$ + Bz1 direct displacement versus impact parameter b. The uncertainties in the displacement $P_r(b)$ are 25−30%.

5.0 kcal for the 1000 K simulations, where 3.0 kcal/mol is $\bar{E}_{rel}$. The uncertainties in the $P_r(b)$ range from 25 to 30%. Given these substantial uncertainties, the substantial structures for the $P_r(b)$ in Figure 5 are not definitive.

Following the procedure outline above, the displacement cross section is 7.5 ± 2.8 $Å^2$ for the 750 K simulation. For the 1000 K simulations at E_{rel} of 1.0, 3.0, and 5.0 kcal/mol, the respective cross sections are 23.9 ± 5.9, 12.4 ± 3.6, and 11.8 ± 3.5 $Å^2$. An E_{rel} displacement cross section is about an order of magnitude smaller than the association cross section. For the 1000 K simulations, $k(E_{rel})$ were calculated from the $\sigma(E_{rel})$ and fit with eq 4, as shown in Figure 4. The fitting parameters are $a = 1.87 \times 10^{-10}$ cm^3/molecule·sec and $b = 0.167$ $(kcal/mol)^{-1}$.

Using eq 6, $k(T)$ for the 750 K simulation is $(4.8 \pm 1.8) \times 10^{-11}$ cm^3/molecule·sec. Using eq 5, and the above fitting parameters gives, $k(T) = (12.2 \pm 3.3) \times 10^{-11}$ cm^3/molecule·sec at 1000 K. The 1000 K $k(T)$ using eq 6 is statistically the same and $(9.4 \pm 2.7) \times 10^{-11}$ cm^3/molecule·sec. The rate constant increases with temperature and, using the 750 and 1000 K $k(T)$ determined from eq 6, the Arrhenius activation energy is 5.6 kcal/mol.

D. Dynamics of $Na^+(Bz)_2$* Dissociation. *1. Simulation Results.* The $Na^+(Bz)_2$* cluster, formed by Bz + $Na^+(Bz) \rightarrow Na^+(Bz)_2$* association, is highly vibrationally/rotationally excited. At 1000 K its total classical energy is 209.2 kcal/mol, which is a sum of the average thermal energies of 87.9 and 93.9 for Bz and $Na^+(Bz)$, which include their zero-point energies (ZPEs), the Bz + $Na^+(Bz)$ collision energy of 3.0 kcal/mol, and the Bz + $Na^+(Bz) \rightarrow Na^+(Bz)_2$ association energy of 24.4 kcal/mol. At 750 K the average $Na^+(Bz)_2$* energy is 186.4 kcal/mol.

Relative populations $N(t)/N(0)$ of the $Na^+(Bz)_2$* clusters versus time for the different impact parameters are given in Figures 6 and 7 for the 750 and 1000 K simulations, respectively. For the 1000 K simulations, all the clusters dissociated within the 90 ps integration time and some of the dissociation involved "total dissociation" for which both Bz molecules dissociated from Na^+. However, for the 750 K simulations, some $Na^+(Bz)_2$* clusters remained when the trajectories were halted at 90 ps, and there were no "total dissociations".

As shown in Figures 6 and 7, there is an initial delay in the $N(t)/N(0)$ plots with a nondissociating component. To fit these distributions versus t it is necessary to shift the simulation $N(t)/N(0)$ to $t = 0$. A nonarbitrary "shifting time" was chosen for each impact parameter by taking the "shifting time" as the average time spent by the associating Bz (i.e., Bz2) within 10 Å of Na^+ for the direct displacement trajectories (Figure 2c) and the direct scattering trajectories for which Bz2 gets close to Na^+ and within 6 Å (Figure 2b). As shown by the shifted $N(t)/N(0)$ in Figures 6 and 7, this procedure identified appropriate "shifting times".

The shifted $N(t)/N(0)$ are excellently fit by the biexponential function

$$N(t)/N(0) = f_1 \exp(-k_1 t) + f_2 \exp(-k_2 t) \quad (8)$$

which is illustrated in Figures 6 and 7. The fit has a constraint of $f_1 + f_2 = 1$. The f and k fitting parameters are listed in Table 1. Overall, the k values are larger at 1000 K, but their difference with the 750 K values is not striking. At 750 K, the k_1 are 5−10 times larger than the k_2. At 1000 K, the k_1/k_2 ratio is similar and 5−8. The nonexponential $N(t)/N(0)$ distributions are expected as the result of the initial nonrandom excitation of the $Na^+(Bz)_2$* cluster by Bz + $Na^+(Bz)$ association.[54,55]

As discussed above, the clusters that are formed can dissociate one or both of the Bz molecules, or remain intact when the trajectories are halted at 90 ps. Of interest is to compare the dissociation probability for the benzene molecule Bz2, which associates to form the cluster with that for Bz1 which was initially attached to Na^+, i.e., the association reaction is Bz2 + $Na^+(Bz1)$. These probabilities are given in Figures 8 and 9 for the 750 and 1000 K simulations, and for the events in which only one benzene molecule dissociates versus time. The dissociation probabilities at time t are given as the total number of dissociations of Bz1 or Bz2 at t divided by the total number of clusters formed. The difference between unity and the sum of the long-time Bz1 and Bz2 dissociation probabilities is the sum of the probability that both Bz molecules dissociate and the probability the cluster remains intact when the trajectory is halted at 90 ps.

Figures 8 and 9 show that there is not a major difference in the dissociation probabilities for the Bz1 and Bz2 molecules. Since energy is released into the Na^+-Bz2 bond when Bz2 associates, it might be expected that Bz2 would have the higher dissociation probability. However, this is not the case. For the 750 K simulations, with impact parameters of 0 and 6 Å, it is Bz1 that has the significantly higher dissociation probability. Bz2 does not have a significantly higher dissociation probability at short times for any of the simulations.

2. Comparison with Previous Simulations of Randomly Excited $Na^+(Bz)_2$ Clusters.* In a previous chemical dynamics simulation,[42] the classical unimolecular dynamics of randomly excited $Na^+(Bz)_2$* was studied. With random initial conditions, the cluster dissociated with an exponential probability versus time, in accord with RRKM theory. The total $Na^+(Bz)_2$* energies considered in these simulations are 164.5, 191.9, 219.4, and 246.8 kcal/mol, for which the respective microcanonical rate constants for the exponential decomposition are 0.013, 0.030, 0.063, and 0.105 ps^{-1}. For the current study, $Na^+(Bz)_2$* is nonrandomly excited at total energies of 186.4 and 209.2 kcal/mol by $Na^+(Bz)$ + Bz association. Interpolating the above energies and rate constants from the previous study yields microcanonical rate constants of 0.027 and 0.051 ps^{-1} for the energies of 186.4 and 209.2 kcal/mol.

As discussed above, the dissociation probabilities $N(t)/N(0)$, for the nonrandomly excited $Na^+(Bz)_2$* clusters in the current

DOI: 10.1021/acs.jpca.5b01922
J. Phys. Chem. A XXXX, XXX, XXX−XXX

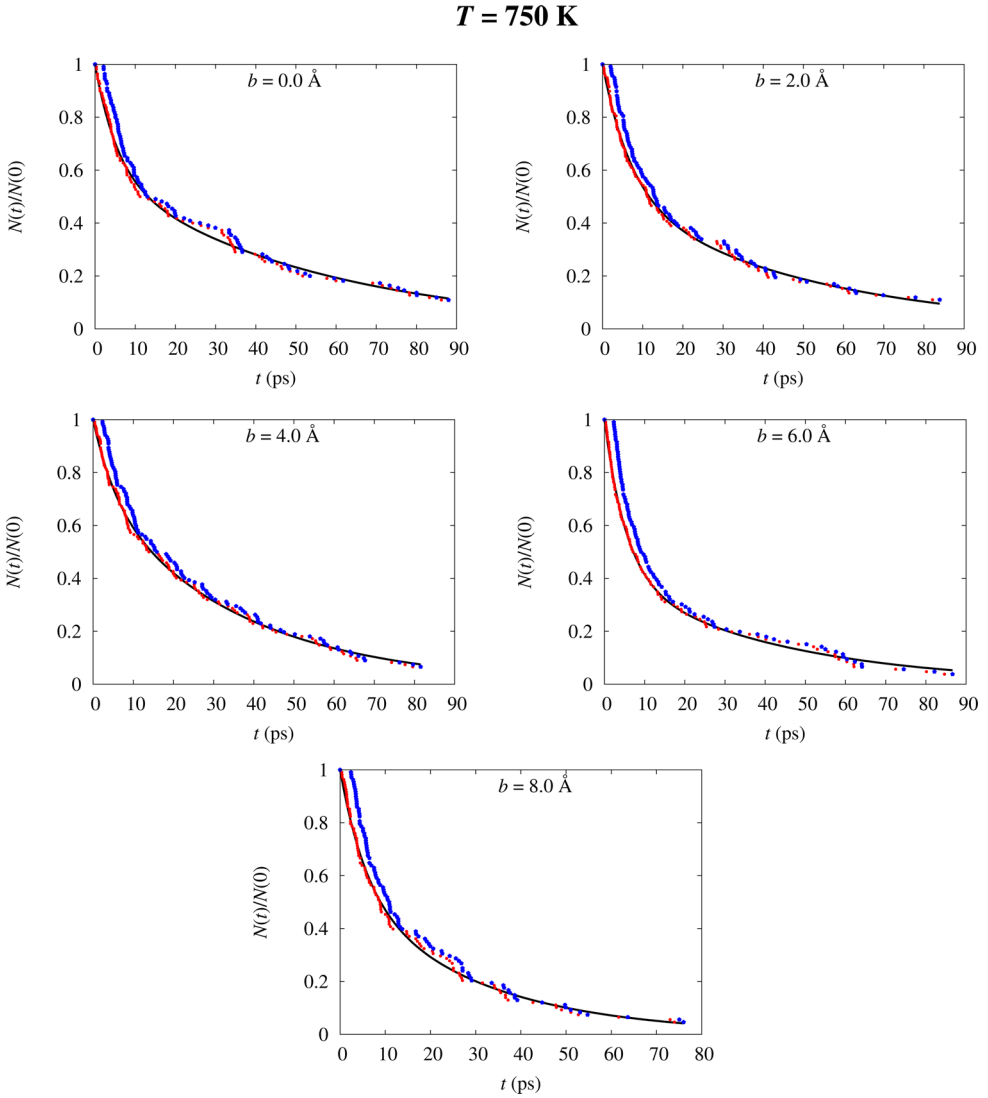

Figure 6. Relative population, $N(t)/N(0)$, of $Na^+(Bz)_2$* clusters versus time for the 750 K simulations at different collision impact parameters. The blue and red points are the simulation and shifted $N(t)/N(0)$, respectively. The black curve is the fit to the shifted $N(t)/N(0)$ with the biexponential function in eq 8. $Na^+(Bz)$ has a 750 K Boltzmann distribution of vibrational and rotational energies for $Na^+(Bz)$ + Bz → $Na^+(Bz)_2$* association. E_{rel} is 2.2 kcal/mol for the association simulation, which is the average E_{rel} at 750 K.

study are well fit by a biexponential function with the k_2 rate constant ~10 times smaller than k_1; see Table 1. It is of interest to see whether k_2, for the long-time component of $N(t)/N(0)$, agrees with the above interpolated microcanonical rate constant. For the current 750 K simulation, with total energy of 186.4 kcal/mol, the fraction of the long-time component for the different impact parameters varies from 0.41−0.72 and k_2 varies from 0.018−0.034 ps^{-1}. The interpolated microcanonical rate constant of 0.027 ps^{-1} is consistent with this range of values. Similarly, the k_2 values for the 1000 K simulations (total energy of 209.2 kcal/mol) are consistent with the interpolated microcanonical rate constant of 0.051 ps^{-1}. For the impact parameters with a long-time component of 0.23 and longer, k_2 varies from 0.028−0.057.

The above analysis indicates that, though the nonrandomly excited $Na^+(Bz)_2$* clusters initially dissociate with a rate constant larger than the RRKM microcanonical value, at long times the rate constant agrees with the RRKM prediction. Such dynamics occur when the initial nonrandom ensemble of $Na^+(Bz)_2$* clusters undergoes intramolecular vibrational energy redistribution (IVR) to form a microcanonical ensemble.[58−60] The relaxation time for IVR is then expected to be shorter than the RRKM lifetime which ranges from 20−37 ps. That the long-time dissociation of nonrandomly excited $Na^+(Bz)_2$* agrees with RRKM theory is consistent with the previous simulation study, for which a microcanonical ensemble of $Na^+(Bz)_2$* has intrinsic RRKM dynamics[58] and dissociates exponentially with the RRKM rate constant.

3. Coupled Phase Space Model for Nonexponential Dissociation. In previous work, Marcus et al.[61] presented a coupled phase space model for describing the type of nonstatistical unimolecular dynamics found here. The model was recently considered for a S_N2 ion−molecule intermediate.[62] It consists of two phase space regions 1 and 2 with state densities of N_1 and N_2. Region 1 is populated by the excitation step, which is $Na^+(Bz)$ + Bz → $Na^+(Bz)_2$* association for the current study. The intramolecular relaxation and unimolecular dissociation processes are

$$\text{Excitation} \rightarrow N_1 \qquad (9a)$$

DOI: 10.1021/acs.jpca.5b01922
J. Phys. Chem. A XXXX, XXX, XXX−XXX

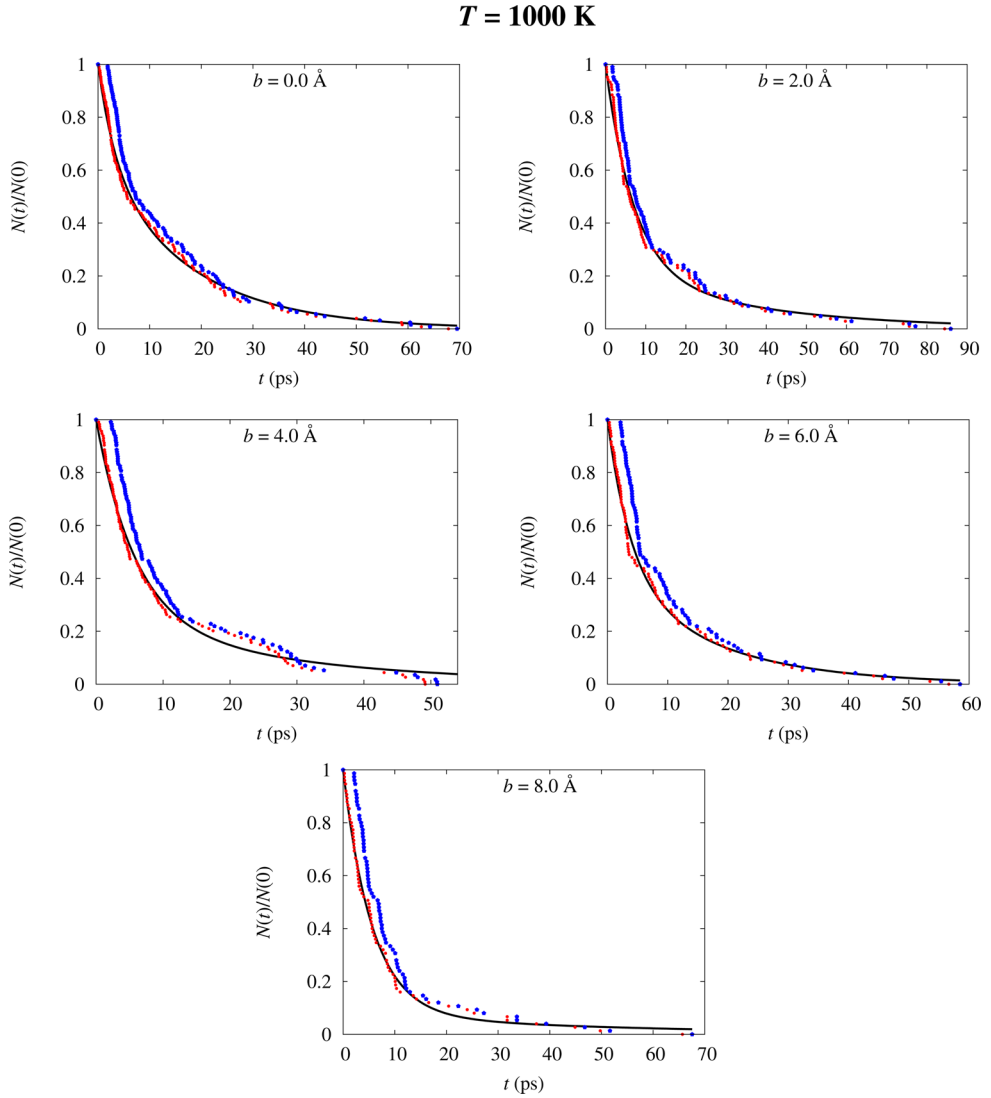

Figure 7. Same as Figure 6, but for the 1000 K simulations. E_{rel} is 3.0 kcal/mol.

Table 1. Parameters for Fits to the $N(t)/N(0)$ Distributions[a]

	fitting parameters[b]			
b[c]	f_1	f_2	k_1	k_2
		750 K		
0	0.41	0.59	0.181	0.018
2	0.49	0.51	0.141	0.020
4	0.28	0.72	0.180	0.028
6	0.59	0.41	0.187	0.024
8	0.45	0.55	0.174	0.034
		1000 K		
0	0.36	0.64	0.301	0.057
2	0.77	0.23	0.145	0.028
4	0.75	0.25	0.173	0.035
6	0.58	0.42	0.258	0.057
8	0.92	0.08	0.178	0.021

[a]The collision energy is $3RT/2$. [b]The rate constants k are in the units of ps^{-1}. [c]The impact parameter b is in the unit of angstroms.

$$N_1 \underset{k_c}{\overset{k_b}{\rightleftharpoons}} N_2 \tag{9b}$$

$$N_1 \xrightarrow{k_a} \text{products} \tag{9c}$$

where k_b and k_c are IVR rate constants. The $t = 0$ initial populations of the two phase space regions are $N_1(0) = N(0)$ and $N_2(0) = 0$. The total number of excited molecules versus time is $N(t) = N_1(t) + N_2(t)$, and is biexponential and given by

$$N(t)/N(0) = [(k_a - \lambda_2)e^{-\lambda_1 t} - (k_a - \lambda_1)e^{-\lambda_2 t}]/(\lambda_1 - \lambda_2) \tag{10}$$

where λ_1 and λ_2 are the eigenvalues for the linear system in eqs 9b and 9c, and satisfy

$$\lambda_1 + \lambda_2 = k_a + k_b + k_c \quad \lambda_1\lambda_2 = k_a k_c \tag{11}$$

The parameters for the biexponential in eq 10 are related to f_1, f_2, k_1, and k_2 in eq 8, i.e., $\lambda_1 = k_1$, $\lambda_2 = k_2$, and $f_1 = (k_a - k_2)/(k_1 - k_2)$. Using the parameters in Table 1, two representative sets of k_a, k_b, and k_c in ps^{-1} are those for the 1000 K simulations with b of 4 and 8 Å: i.e., $b = 4$ Å, $k_a = 0.139$, $k_b = 0.026$, and $k_c = 0.044$; and $b = 8$ Å, $k_a = 0.165$, $k_b = 0.011$, and $k_c = 0.023$. For all five 1000 K simulations in Table 1, k_a ranges from 0.118 to 0.174, k_b from 0.011 to 0.095, and k_c from 0.022 to 0.118; and for the 750 K simulations, these ranges are k_a from 0.071 to 0.120, k_b from 0.046 to 0.076, and k_c from 0.036 to 0.071. Given the

DOI: 10.1021/acs.jpca.5b01922
J. Phys. Chem. A XXXX, XXX, XXX−XXX

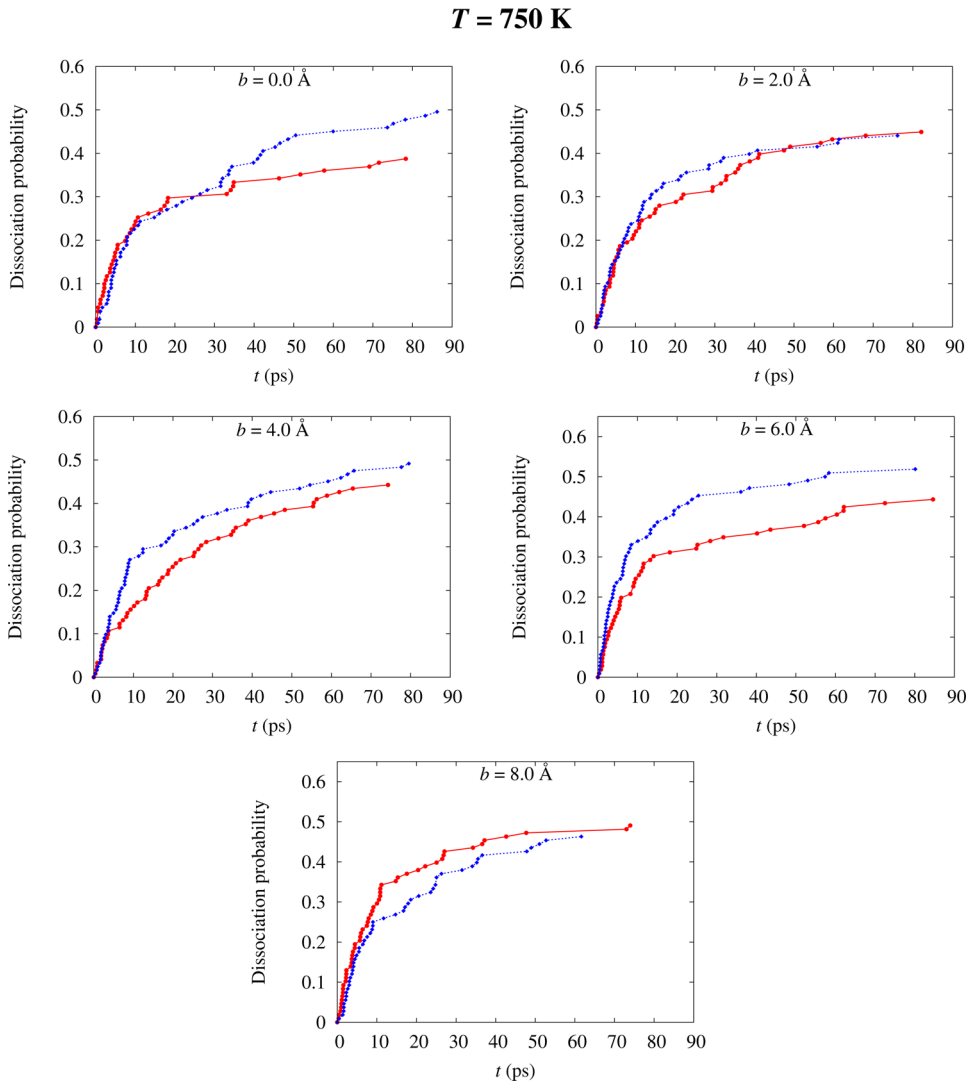

Figure 8. Total dissociation probability versus time for dissociating Bz1 and Bz2 from the $Na^+(Bz)_2$* cluster. Bz2 associates with Na^+(Bz1) to form the cluster. Red points are for Bz2 dissociation and blue points are for Bz1 dissociation. The lines connect the points and are not fits. Simulations are for 750 K. Na^+(Bz) has a 750 K Boltzmann distribution of vibrational and rotational energies for Na^+(Bz) + Bz → Na+$(Bz)_2$* association. E_{rel} is 2.2 kcal/mol for the association simulation, which is the average E_{rel} at 750 K.

nonexponential dissociation, k_a larger than k_b and k_c is expected.[61] The IVR times for k_b, i.e., 1/ k_b, range from 10 to 91 ps and those for k_c range from 8 to 45 ps. These IVR times are similar to, but some are larger than, the RRKM lifetimes of 37 and 20 ps for the respective 750 and 1000 K simulations, given above in Section 2.

The microcanonical RRKM rate constant for the above model is[61]

$$k_{RRKM} = k_a k_c/(k_b + k_c) \quad (12)$$

For the five sets of 750 K simulation parameters in Table 1, values for this k_{RRKM} range from 0.028 to 0.053 ps^{-1} and for the five 1000 K sets of parameters they range from 0.074 to 0.111 ps^{-1}. These k_{RRKM} range from the same as and only two times larger than the microcanonical unimolecular rate constants determined from the simulations and given above. Their values are 0.027 and 0.051 ps^{-1} for the 750 and 1000 K simulations, respectively.

In assessing the coupled phase space model in eqs 9, its significant feature is that it gives the biexponential $Na^+(Bz)_2$* dissociation probability found from the simulation. However, it gives IVR times that seem to be somewhat too large as compared to the intrinsic RRKM dynamics and RRKM, microcanonical rate constant for $Na^+(Bz)_2$* dissociation. However, the model's estimate of the microcanonical rate constant is at most only a factor of 2 to large. Although the model has some shortcomings, overall it gives a good description of the simulation dynamics.

IV. COMPARISON OF CHEMICAL DYNAMICS SIMULATIONS OF ION−MOLECULE ASSOCIATION RATE CONSTANTS

In Table 2, the rate constants calculated for Na^+(Bz) + Bz association are compared with those for other ion−molecule associations, determined from previous chemical dynamics simulations. For these previous studies, the rate constant decreases with increase in temperature as found here for Na^+(Bz) + Bz association. Overall, the rate constants for the different associations are similar, but they increase as the strength of the ion−molecule attractive potential increases; e.g., at 300 K the $Li^+ + H_2O$ rate constant is about 2.5 times larger than that for $K^+ + H_2O$. The association rate constants for Na^+(Bz) + Bz at 750 and 1000 K are similar to that for $Cl^- + CH_3Cl$ at 1000 K.

DOI: 10.1021/acs.jpca.5b01922
J. Phys. Chem. A XXXX, XXX, XXX−XXX

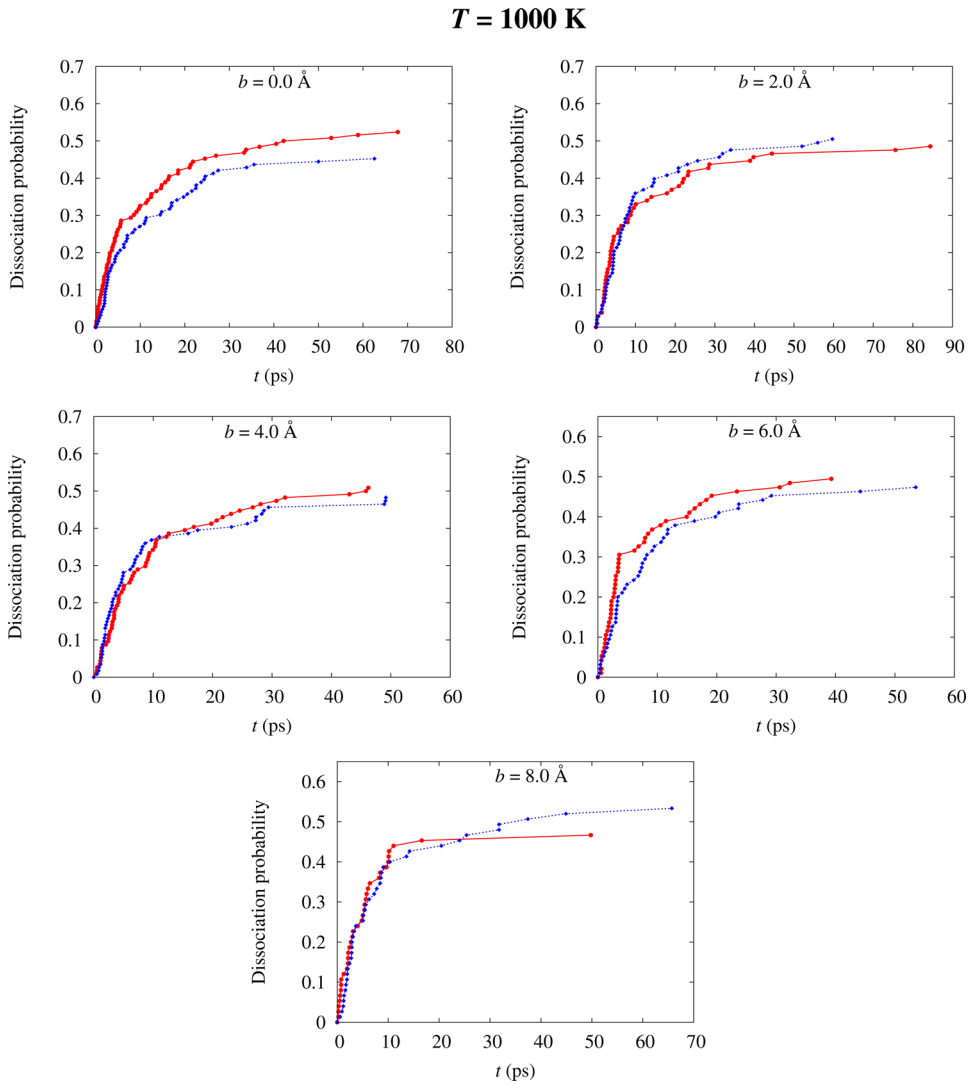

Figure 9. Same as Figure 8, , but for the 1000 K simulations. E_{rel} is 3.0 kcal/mol.

Table 2. Ion−Molecule Association Rate Constants from Chemical Dynamics Simulations

association	T (K)	rate constant[a]	ref.
$K^+ + H_2O$	300	1.3×10^{-9}	36
$Li^+ + H_2O$	300	3.1×10^{-9}	36
$Li^+(H_2O) + H_2O$	300	4.2×10^{-9}	36
$Li^+ + (CH_3)_2O$	200	12.0×10^{-9}	37
	300	8.0×10^{-9}	37[b]
	1000	4.8×10^{-9}	37
$Cl^- + CH_3Cl$	200	2.2×10^{-9}	39
	300	1.7×10^{-9}	39
	500	1.2×10^{-9}	39
	1000	7.0×10^{-10}	39
$Na^+(Bz) + Bz$	750	8.3×10^{-10}	This work
	1000	8.0×10^{-10}	This work

[a]Rate constant is in units of cm^3/molecule.sec. [b]In an earlier study (ref 36), a rate constant of 5.2×10^{-9} cm^3/molecule.sec was reported for $Li^+ + (CH_3)_2O$ at 300 K.

The $Li^+ + (CH_3)_2O$ association rate constant at 1000 K is six times larger than that for $Na^+(Bz) + Bz$.

V. SUMMARY

Chemical dynamics simulations were performed to study $Na^+(Bz) + Bz$ association at 750 and 1000 K to form the vibrationally/rotationally excited $Na^+(Bz)_2$* cluster. The ensuing unimolecular dissociation of this cluster was also investigated. Four trajectory types were found in the simulations, and for two, the colliding Bz molecule directly scattered off $Na^+(Bz)$ without forming a $Na^+(Bz)_2$* cluster. For most of these trajectories, the Na^+−Bz separation for the colliding Bz molecule remained greater than 6.0 Å, without a strong Na^+−Bz interaction. However, for some, the separation became quite small, and the Na^+−Bz interaction was strong. However, the reactant collision energy was not transferred to vibration and/or rotation energy of the $Na^+(Bz) + Bz$ system and a $Na^+(Bz)_2$* cluster was not formed.[36−41,63] The third and fourth trajectory types are formation of the $Na^+(Bz)_2$* cluster and a direct noncluster displacement reaction, for which the colliding Bz molecule directly displaces Bz attached to Na^+; i.e., $Bz + Na^+(Bz) \rightarrow Na^+(Bz) + Bz$.

Cross sections and rate constants were calculated for the $Bz + Na^+(Bz) \rightarrow Na^+(Bz)_2$* association and $Bz + Na^+(Bz) \rightarrow Na^+(Bz) + Bz$ direct displacement reactions. For the association reaction, both the cross section and rate constant decreased as the

DOI: 10.1021/acs.jpca.5b01922
J. Phys. Chem. A XXXX, XXX, XXX−XXX

temperature was increased from 750 to 1000 K. However, the cross section and rate constant increased for the direct displacement reaction with this increase in temperature. At 750 K the cross section for direct displacement is ~20 times smaller than that for association, while this factor is ~10 at 1000 K. The uncertainty in the calculated association cross section is small and only 6−7%. For the displacement cross section, the uncertainty is larger and 25−30%. However, since the displacement reaction makes only a small contribution to the total reaction, its rather large uncertainty does not appreciably affect the uncertainty for the overall reaction rate. The rate constant for Bz + $Na^+(Bz)$ → $Na^+(Bz)_2$* association is consistent with chemical dynamics simulations of rate constants for other ion−molecule associations.[34−41] The Bz + $Na^+(Bz)$ association rate constant at 1000 K is similar to that determined for Cl^- + CH_3Cl association at the same temperature.[39] In a simulation of H_2O + $Li^+(H_2O)$ a direct displacement reaction was found as found here for Bz + $Na^+(Bz)$.[36]

The dissociation probability $N(t)/N(0)$ of the energized $Na^+(Bz)_2$* clusters, prepared by Bz + $Na^+(Bz)$ association, is biexponential. The fractions for the two components in the biexponential are similar in size, with the rate constant for the short-time component approximately an order of magnitude larger than that for longer times. This nonexponential dissociation is a result of the nonrandom excitation of the $Na^+(Bz)_2$* clusters by Bz + $Na^+(Bz)$ association.[58,59] The rate constant for the long-time component agrees with that of RRKM theory, consistent with rapid IVR[60] and intrinsic RRKM[58] unimolecular dynamics. The Bz molecules of the $Na^+(Bz)_2$* cluster have nearly equal dissociation probabilities.

Ion−molecule association is expected to initially preferentially and nonrandomly excite the intermolecular modes of the ion−molecule complex. Vibrational energy will then transfer from the intermolecular to intramolecular modes. For $Na^+(Bz)_2$* this IVR is sufficiently rapid that, if the molecule is excited randomly, its dissociation probability is exponential and in accord with RRKM theory.[42] However, not all ion−molecule complexes have such intrinsic RRKM dynamics. An illustrative example is the Cl^-−CH_3Cl ion−dipole complex for the Cl^- + CH_3Cl S_N2 nucleophilic substitution reaction.[39] For this system there is weak coupling between the intermolecular and intramolecular modes, and, though not quantified, IVR is slow.

The different IVR dynamics for $Na^+(Bz)_2$* and Cl^-−CH_3Cl may be understood by considering their intermolecular and intramolecular vibrational frequencies ν. IVR occurs via resonance pathways and when the number of these pathways and their couplings increase IVR is enhanced.[64] The intermolecular ν values for $Na^+(Bz)_2$* range from 40 to 271 cm^{-1}, while the Bz intramolecular ν values are as low as 400 and 613 cm^{-1}. Thus, there are low-order resonance conditions for IVR in $Na^+(Bz)_2$*. By contrast, there are no low-order resonance conditions for IVR in Cl^-−CH_3Cl. The three intermolecular frequencies are 71(2) and 101 cm^{-1} and the lowest CH_3Cl intramolecular frequency is the 783 cm^{-1} C−Cl stretch.[39] Thus, IVR for ion−molecule complexes may be qualitatively understood by considering resonance conditions between the intermolecular and intramolecular modes of the complex.

AUTHOR INFORMATION

Notes

The authors declare no competing financial interest.

ACKNOWLEDGMENTS

The work presented here is a part of project supported by the Air Force Office of Scientific Research (AFOSR) under grant No. FA9550-12-1-0472. The Robinson computer cluster in the TTU Department of Chemistry and Biochemistry, whose purchase was funded by the National Science Foundation CRIF-MU Grant CHE-0840493, was used for the computations. We wish to thank Jing Xie for her important assistance.

REFERENCES

(1) Sloan, G. C.; Hayward, T. L.; Allamandola, L. J.; Bregman, J. D.; Devito, B.; Hudgins, D. M. Direct Spectroscopic Evidence for Ionized Polycyclic Aromatic Hydrocarbons in the Interstellar Medium. *Astrophys. J. Lett.* **1999**, *513*, L65−L68.
(2) Léger, A.; Puget, J. L. Identification of the "Unidentified" IR Emission Features of Interstellar Dust? *Astron. Astrophys.* **1984**, *137*, L5−L8.
(3) Allamandola, L. J.; Tielens, A. G. G. M.; Barker, J. R. Polycyclic Aromatic Hydrocarbons and the Unidentified Infrared Emission Bands. *Astrophys. J. Lett.* **1985**, *290*, L25−L28.
(4) Serra, G.; Chaudret, B.; Saillard, Y. Organic Chemistry in Interstellar Medium. *Astron. Astrophys.* **1992**, *260*, 489−493.
(5) Marty, P.; Serra, G.; Chaudret, B.; Ristorcelli, I. Iron-Aromatics Coordination in Molecular Clouds. *Astron. Astrophys.* **1994**, *282*, 916−923.
(6) Fordyce, J. S.; Sheibley, D. W. Estimate of Contribution of Jet Aircraft Operations to Trace Element Concentration at or Near Airports. *J. Air Pollut. Control Assoc.* **1975**, *25*, 721−724.
(7) Pande, S. G.; Hardy, D. R. Effect of Copper, MDA, and Accelerated Aging on Jet Fuel Thermal Stability As Measured by the Gravimetric JFTOT. *Energy Fuel.* **1995**, *9*, 177−182.
(8) Edwards, T. Cracking and Deposition Behavior of Supercritical Hydrocarbon Aviation Fuels. *Combust. Sci. Technol.* **2006**, *178*, 307−334.
(9) Altin, O.; Eser, S. Analysis of Solid Deposits from Thermal Stressing of a JP-8 Fuel on Different Superalloy Surfaces in a Flow Reactor. *Ind. Eng. Chem. Res.* **2001**, *40*, 589−595.
(10) Ianovski, L. S. Endothermic Fuels for Hypersonic Aviation. *AGARD Conference on Fuels and Combustion Technology for Advanced Aircraft Engines, AGARD CP-536* **1993**, 44-1−44-8.
(11) Edwards, T.; Anderson, S. *Results of High Temperature JP-7 Cracking Assessment*; AIAA Paper 93-0806, 1993.
(12) Maurice, L. Q.; Striebich, R. C.; Edwards, T. *Formation of Cyclic Compounds in the Fuel Systems of Hydrocarbon Fueled High Speed Vehicles.* AIAA Paper 98-3534, 1998.
(13) Stewart, J. F.; Brezinsky, K.; Glassman, I. Supercritical Methylcyclohexane Pyrolysis: A Flow Reactor Study. *ACS Petrol. Chem. Div. Preprints* **1998**, *43*, 433−437.
(14) Maurice, L. Q.; Striebich, R. C.; Edwards, T. Cyclic Species Formation in the Fuel Systems of High-Speed Vehicles. *ACS Petrol. Chem. Div. Preprints* **1998**, *43*, 423−427.
(15) Dougherty, D. A. Cation-π Interactions in Chemistry and Biology: A New View of Benzene, Phe, Tyr, and Trp. *Science* **1996**, *271*, 163−168.
(16) Ma, J. C.; Dougherty, D. A. The Cation−π Interaction. *Chem. Rev.* **1997**, *97*, 1303−1324.
(17) Gallivan, J. P.; Dougherty, D. A. Cation−π Interactions in Structural Biology. *Proc. Natl. Acad. Sci. U. S. A.* **1999**, *96*, 9459−9464.
(18) Minoux, H.; Chipot, C. Cation−π Interactions in Proteins: Can Simple Models Provide an Accurate Description? *J. Am. Chem. Soc.* **1999**, *121*, 10366−10372.
(19) Grohima, M. M.; Santhosh, C.; Ahmad, S. Structural Analysis of Cation−π Interactions in DNA Binding Proteins. *Int. J. Biol. Macromol.* **2004**, *34*, 203−211.
(20) Crowley, P. B.; Golovin, A. Cation−π Interactions in Protein−Protein Interfaces. *Proteins* **2005**, *59*, 231−239.
(21) Wu, R.; McMahon, T. B. Investigation of Cation−π Interactions in Biological Systems. *J. Am. Chem. Soc.* **2008**, *130*, 12554−12555.

DOI: 10.1021/acs.jpca.5b01922
J. Phys. Chem. A XXXX, XXX, XXX−XXX

(22) Caldwell, J. W.; Kollman, P. A. Cation−π Interactions: Nonadditive Effects Are Critical in Their Accurate Representation. *J. Am. Chem. Soc.* **1995**, *117*, 4177−4178.
(23) Mecozzi, S.; West, A. P.; Dougherty, D. A. Cation−π Interactions in Simple Aromatics: Electrostatics Provide a Predictive Tool. *J. Am. Chem. Soc.* **1996**, *118*, 2307−2308.
(24) Armentrout, P. B.; Rodgers, M. T. An Absolute Sodium Cation Affinity Scale: Threshold Collision-Induced Dissociation Experiments and *Ab initio* Theory. *J. Phys. Chem. A* **2000**, *104*, 2238−2247.
(25) Amicangelo, J. C.; Armentrout, P. B. Absolute Binding Energies of Alkali-Metal Cation Complexes with Benzene Determined by Threshold Collision-Induced Dissociation Experiments and *Ab initio* Theory. *J. Phys. Chem. A* **2000**, *104*, 11420−11432.
(26) Tan, X.; Zhu, W. L.; Cui, M.; Luo, X. M.; Gu, J. D.; Silman, I.; Sussman, J. L.; Jiang, H. L.; Ji, R. Y.; Chen, K. X. Noncovalent Interaction or Chemical Bonding Between Alkaline Earth Cations and Benzene? A Quantum Chemistry Study Using MP2 and Density-Functional Theory Methods. *Chem. Phys. Lett.* **2001**, *349*, 113−122.
(27) Tsuzuki, S.; Yoshida, M.; Uchimaru, T.; Mikami, M. The Origin of the Cation/π Interaction: The Significant Importance of the Induction in Li^+ and Na^+ Complexes. *J. Phys. Chem. A* **2001**, *105*, 769−773.
(28) Soteras, I.; Orozco, M.; Luque, F. J. Induction Effects in Metal Cation−Benzene Complexes. *Phys. Chem. Chem. Phys.* **2008**, *10*, 2616−2624.
(29) Marshall, M. S.; Steele, R. P.; Thanthiriwatte, K. S.; Sherrill, C. D. Potential Energy Curves for Cation−π Interactions: Off-Axis Configurations are Also Attractive. *J. Phys. Chem. A* **2009**, *113*, 13628−13632.
(30) Jaeger, T. D.; Heijnsbergen, D. v.; Klippenstein, S. J.; Helden, G. v.; Meijer, G.; Duncan, M. A. Vibrational Spectroscopy and Density Functional Theory of Transition-Metal Ion-Benzene and Dibenzene Complexes in the Gas Phase. *J. Am. Chem. Soc.* **2004**, *126*, 10981−10991.
(31) Yi, H. B.; Lee, H. M.; Kim, K. S. Interaction of Benzene with Transition Metal Cations: Theoretical Study of Structures, Energies, and IR Spectra. *J. Chem. Theory Comput.* **2009**, *5*, 1709−1719.
(32) Mahadevi, A. S.; Sastry, G. N. Cation−π Interaction: Its Role and Relevance in Chemistry, Biology, and Material Science. *Chem. Rev.* **2013**, *113*, 2100−2138.
(33) Kolakkandy, S.; Pratihar, S.; Aquino, A. J. A.; Wang, H.; Hase, W. L. Properties of Complexes Formed by Na^+, Mg^{2+}, and Fe^{2+} Binding with Benzene Molecules. *J. Phys. Chem. A* **2014**, *118*, 9500−9511.
(34) Hase, W. L.; Feng, D.-F. Dynamics of Ion Solvation. $Li^+ + H_2O \rightarrow Li^+(H_2O)^*$. *J. Chem. Phys.* **1981**, *75*, 738−744.
(35) Swamy, K. N.; Hase, W. L. Dynamics of Ion−Molecule Recombination. II. An Alkali Ion and a Water Molecule. *J. Chem. Phys.* **1982**, *77*, 3011−3021.
(36) Swamy, K. N.; Hase, W. L. Dynamics of Ion−Molecule Recombination. III. Trends in the Recombination Efficiency. *J. Am. Chem. Soc.* **1984**, *106*, 4071−4077.
(37) Vande Linde, S. R.; Hase, W. L. Dynamics of Ion−Molecule Recombination. IV. $Li^+ + (CH_3)_2O$ Association. *Comput. Phys. Commun.* **1988**, *51*, 17−34.
(38) Hase, W. L.; Darling, C. L.; Zhu, L. Dynamics of Ion−Molecule Recombination. V. A Study of Energy Transfer Pathways. *J. Chem. Phys.* **1992**, *96*, 8295−8306.
(39) Vande Linde, S. R.; Hase, W. L. Trajectory Studies of S_N2 Nucleophilic Substitution. I. Dynamics of $Cl^- + CH_3Cl$ Reactive Collisions. *J. Chem. Phys.* **1990**, *93*, 7962−7980.
(40) Hase, W. L. S_N2 Reactions and Their Double-Well Potentials. In *Encyclopedia of Mass Spectrometry, Fundamentals of and Applications to Organic (and Organometallic) Compounds*; Gross, M., Caprioli, R., Nibbering, N. M. N., Eds.; Elsevier Science: New York, 2004; Vol. *5*, 504−515.
(41) Hase, W. L.; Wang, H.; Peslherbe, G. H. Dynamics of Gas-Phase S_N2 Nucleophilic Substitution Reactions. In *Advances in Gas Phase Ion Chemistry*; Babcock, L. M., Adams, N. G., Eds.; JAI Press: Greenwich, CT, 1998; Vol. 3, 125−156.
(42) Kolakkandy, S.; Paul, A. K.; Pratihar, S.; Kohale, S. C.; Barnes, G. L.; Wang, H.; Hase, W. L. Energy and Temperature Dependent Dissociation of the $Na^+(Benzene)_{1,2}$ Clusters: Importance of Anharmonicity. *J. Chem. Phys.* **2015**, *142*, 044306.
(43) Lenzer, T.; Luther, K.; Troe, J.; Gilbert, R. G.; Lim, K. F. Trajectory Simulations of Collisional Energy Transfer in Highly excited Benzene and Hexafluorobenzene. *J. Chem. Phys.* **1995**, *103*, 626−641.
(44) George, A. V.; Field, L. D.; Hambley, T. W. *The Essentials of Organic Chemistry*; Prentice Hall: Sydney, 1996.
(45) Zou, W.; Kalescky, R.; Kraka, E.; Cremer, D. Relating Normal Vibrational Modes to Local Vibrational Modes: Benzene and Naphthalene. *J. Mol. Model.* **2013**, *19*, 2865−2877.
(46) McMillen, D. F.; Golden, D. M. Hydrocarbon Bond Dissociation Energies. *Annu. Rev. Phys. Chem.* **1982**, *33*, 493−532.
(47) Rashev, S. On the Empirical Determination of Some Harmonic and Anharmonic Force Constants in Benzene. *J. Phys. Chem. A* **2001**, *105*, 6499−6505.
(48) Jorgensen, W. L.; Severance, D. L. Aromatic−aromatic interactions: Free energy profiles for the benzene dimer in water, chloroform, and liquid benzene. *J. Am. Chem. Soc.* **1990**, *112*, 4768.
(49) Lee, E. C.; Kim, D.; Jurecka, P.; Tarakeswar, P.; Hobza, P.; Kim, S. Understanding of Assembly Phenomena by Aromatic−Aromatic Interactions: Benzene Dimer and the Substituted Systems. *J. Phys. Chem. A* **2007**, *111*, 3446.
(50) Deb, B.; Hu, W.; Song, K.; Hase, W. L. An Analytic Potential Energy Function to Model Protonated Peptide Soft-Landing Experiments. The $CH_3NH_3^+/CH_4$ Interaction. *Phys. Chem. Chem. Phys.* **2008**, *10*, 4565−4572.
(51) Pratihar, S.; Kohale, S.; Vázquez, S.; Hase, W. L. *J. Phys. Chem. B* **2014**, *118*, 5577−5588.
(52) Hase, W. L.; Duchovic, R. J.; Hu, X.; Kormonicki, A.; Lim, K.; Lu, D.-H.; Peslherbe, G. H.; Swamy, K. N.; Vande Linde, S. R.; Varandas, A. J. C.; Wang, H.; Wolfe, R. J. A General Chemical Dynamics Computer Program. *Quantum Chemistry Program Exchange (QCPE) Bulletin* **1996**, *16*, 671.
(53) Hu, X.; Hase, W. L.; Pirraglia, T. Vectorization of the General Monte Carlo Classical Trajectory Program VENUS. *J. Comput. Chem.* **1991**, *12*, 1014−1024.
(54) Peslherbe, G. H.; Wang, H.; Hase, W. L. Monte Carlo Sampling for Classical Trajectory Simulations. *Adv. Chem. Phys.* **1999**, *105*, 171−201.
(55) Schlier, C.; Seiter, A. High-Order Symplectic Integration: An Assessment. *Comput. Phys. Commun.* **2000**, *130*, 176−189.
(56) Gilbert, R. G.; Smith, S. C. *Theory of Unimolecular and Recombination Reactions*; Blackwell: Oxford, 1990.
(57) Baer, T.; Hase, W. L. Unimolecular Reaction Dynamics. *Theory and Experiments*; Oxford: New York, 1996.
(58) Bunker, D. L.; Hase, W. L. On Non-RRKM Unimolecular Kinetics: Molecules in General and CH_3NC in Particular. *J. Chem. Phys.* **1973**, *59*, 4621−4632.
(59) Hase, W. L.; Buckowski, D. G.; Swamy, K. N. Dynamics of Ethyl Radical Decomposition. III. Effect of Chemical Activation versus Microcanonical Sampling. *J. Phys. Chem.* **1983**, *87*, 2754−2763.
(60) Hase, W. L. Unimolecular and Intramolecular Dynamics: Relationship to Potential Energy Surface Properties. *J. Phys. Chem.* **1986**, *90*, 365−374.
(61) Marcus, R. A.; Hase, W. L.; Swamy, K. N. RRKM and Non-RRKM Behavior in Chemical Activation Studies. *J. Phys. Chem.* **1984**, *88*, 6717−6720.
(62) Paranjothy, M.; Sun, A.; Paul, A. K.; Hase, W. L. Models for Intrinsic Non-RRKM Unimolecular Dynamics. Decomposition of the S_N2 Intermediate $Cl^-−CH_3Br$. *Z. Phys. Chem.* **2013**, *227*, 1361−1379.
(63) Hase, W. L.; Cho, Y. J. Trajectory Studies of S_N2 Nucleophilic Substitution. III. Dynamical Stereochemistry and Energy Transfer Pathways for the $Cl^- + CH_3Cl$ Association and Direct Substitution Reactions. *J. Chem. Phys.* **1993**, *98*, 8626−8639.
(64) Oxtoby, D. W.; Rice, S. A. Nonlinear Resonance and Stochasticity in Intramolecular Energy Exchange. *J. Chem. Phys.* **1976**, *65*, 1676−1683.

DOI: 10.1021/acs.jpca.5b01922
J. Phys. Chem. A XXXX, XXX, XXX−XXX